Espaço & Geografia, vol.24, n.1 (2021), 132:148
ISSN: 1516-9375

THE SENSITIVITY OF EVAPOTRANSPIRATION FOR LAND USES AND TOPOGRAPHY IN AREA OF CERRADO BIOME – BRAZIL

A SENSIBILIDADE DA EVAPOTRANSPIRAÇÃO PARA USOS DO SOLO E TOPOGRAFIA EM ÁREA DO BIOMA CERRADO – BRASIL

Lucas Augusto Pereira da Silva[1], Édson Luís Bolfe[2], Cristiano Marcelo Pereira de Souza[3], Roberto Filgueiras[4]

[1]Universidade Federal de Uberlândia
Doutorando no Programa de Pós-Graduação em Geografia – PPGEO/UFU
Av. João Naves de Ávila, 2121 - Santa Mônica, Uberlândia - MG, 38408-100 - Brasil
E-mail: lucasagusto@ufu.br

[2]Embrapa Secretaria de Inteligência e Relações Estratégicas
Av. Sd. Passarinho, 303 - Jardim Chapadão, Campinas – SP - Brasil.
E-mail: edson.bolfe@embrapa.br

[3]Universidade Estadual de Montes Claros
Programa de Pós Graduação em Geografia – PPGEO/UNIMONTES
Campus Universitário Prof. Darcy Ribeiro, Av. Prof. Rui Braga, s/n - Vila Mauriceia, Montes Claros - MG, 39401-089 - Brasil
Claros – MG. E-mail: cristiano.souza@ufv.br

[4]Universidade Federal de Viçosa
Programa de Pós-Graduação em Engenharia Agrícola – POSDEA/UFV
Departamento de Engenharia Agricola, Bela Vista, Viçosa - MG, 36570-000 - Brasil
Email: roberto.f.filgueiras@ufv.br

Recebido em 20 de janeiro de 2021, Aceito em 08 de junho de 2021

Abstract: Evapotranspiration (ET) is a crucial element in the spatiotemporal dynamics of moisture, energy, and heat, and is related to climatic, pedogeomorphological, and phytophysiognomic aspects of the landscape. Therefore, estimating ET requires dynamic and integrated temporal analysis with biophysical landscape factors. The study aimed to analyze the behavior of ET through the analysis of land use and land cover and topographic in time series. The Simple Algorithm for Evapotranspiration Recovery (SAFER) model was used to obtain the variable ET in the periods of 01/21, 02/22, 05/13 and 06/30/2019 (variables). A database of explanatory covariates was constructed, including land use and land cover, satellite image data (Landsat-8) and digital elevation model (SRTM). The values of variables and covariates were extracted into a grid of points and separated for three altimetric conditions, and the linear Gaussian Models (GLM) were applied to the point data. The most explanatory spectral covariates for the ET variation were Albedo and Surface Temperature. And the covariates related to topography were Digital Elevation Model and Topographic Moisture Index. In general, the wet period presents a higher ET rate (2.06 mm d^{-1}). Forests generated the highest ET regardless of period (1.62 mm d^{-1} to 4.03 mm d^{-1}). Elevated topography also influences the increase in ET in relation to the same lower altimetry classes (A2 and A3). This influence is associated with the altitude dynamics and intrinsic elements of the region, such as the marshy environment in the A3 region, where the highest ET values occurred. This work stands out from its peers for addressing the influence of landscape aspects on the knowledge of evapotranspiration variation, a vanguard theme in the scope of spatial analysis.

Keywords: Remote Sensing, SAFER, GLM, and hypsometric regions.

Resumo: A evapotranspiração (ET) é um elemento crucial na dinâmica espaço-temporal de umidade, energia e calor, e está relacionada a aspectos climáticos, pedogeomorfológicos e fitofisionômicos da paisagem. Portanto, estimar ET requer análise temporal dinâmica e integrada com fatores biofísicos da paisagem. O estudo teve como objetivo analisar o comportamento do ET por meio da análise do uso e cobertura do solo e da topográficas em série temporal. O modelo Algoritmo Simples para Recuperação da Evapotranspiração (SAFER) foi utilizado para obter a variável ET nos períodos de 21/01, 22/02, 13/05 e 30/06/2019 (variáveis). Um banco de dados de covariáveis explicativas foi construído, incluindo uso e cobertura do solo, dados de imagem de satélite (Landsat-8) e modelo digital de elevação (SRTM). Os valores das variáveis e covariáveis foram extraídos para uma grade de pontos e separados para três condições altimétricas, e nos dados pontuais foram aplicados os Modelos Lineares Gaussianos (GLM). As covariáveis espectrais mais explicativas para a variação de ET foram Albedo e Temperatura da Superfície. E as covariáveis relacionadas à topografia foram Modelo Digital de Elevação e Índice de Umidade Topográfica. Em geral, o período úmido apresenta maior taxa de ET (2,06 mm d^{-1}). As Florestas geraram a maior ET independente do período (1,62 mm d^{-1} a 4,03 mm d^{-1}). A topografia elevada também influencia no aumento do ET em relação às mesmas classes de altimetria inferior (A2 e A3). Essa influência está associada à dinâmica de altitude e a elementos intrínsecos da região, como o ambiente pantanoso na região A3, onde ocorreram os maiores valores de ET. Este trabalho destaca-se dos pares por abordar a influência de aspectos da paisagem no conhecimento da variação da evapotranspiração, tema de vanguarda no âmbito da análise espacial.

Palavras-Chave: Sensoriamento Remoto, SAFER, GLM e Regiões Altimétricas.

INTRODUCTION

Evapotranspiration (ET) is a crucial element in the space-time dynamics of humidity, energy, and heat. ET is a dynamic variable, and in addition to the temporal aspect, it is related to climatic, pedogeomorphological, and phytophysiognomic factors of the landscape (MELESSE et al., 2007; ANDERSON et al., 2012; RUHOFF et al., 2013). ET data has applications in studies of environmental scenarios (WANG et al., 2013), hydrological models (IMMERZEEL; DROOGERS, 2008), and watershed management. However, some studies consider only the phenological and structural context as response covariable (SENAY, 2008; SACKS; KUCHARIK, 2011).

Studies that address ET variation and landscape elements' association use radiation and energy balance methods (HEMAKUMARA; CHANDRAPALA; MOENE, 2003; KIPTALA et al., 2013; PÔÇAS et al., 2013). The disadvantage of this method is the need for many physical interactions, obtaining anchor pixels (SILVA; CASTRO TEIXEIRA; MANZIONE, 2019) and uncertainties in obtaining heat flows (especially sensible heat), with overestimates about field data (MARX et al., 2008; SCHERER-WARREN, 2012). Alternatively, the more directs and simplified models overcome this problem (SILVA; CASTRO TEIXEIRA; MANZIONE, 2019). In the last decade, the use of the Simple Algorithm for Evapotranspiration Recovery (SAFER) empirical model has grown; with efficiency in several ecosystems, covering the phenological variation of different phytophysiognomies, energy availability, temperature behavior and water maintenance in the environment through evapotranspiration (ALTHOFF et al., 2019; CASTRO TEIXEIRA et al., 2020; MUSSI et al., 2020a; SANTOS et al., 2020b).

In Brazil, the Cerrado Biome is an example of landscape heterogeneity, a determining factor for ET variation (ARANTES; FERREIRA; COE, 2016). The heterogeneity of the cerrado is evident in the state of Minas Gerais, as it places a condition of geodiversity, with the geology of the Archean and Phanerozoic ages, in the most diverse tectonic and metamorphic contexts, which they form sustain a pedogeomorphological diversity (SILVA et al., 2018). Besides, the geoecological arrangement of Minas Gerais results from the crossing of three biomes, with limits not well defined, configuring itself in several regions as a morphoclimatic transition domain (AB'SABER, 1970). In this scenario, the Pandeiros River Protection Area (EPA-RP) is inserted, with the presence of mosaics of natural vegetation cover and anthropic uses, object of interest to several researchers, aiming at understanding the physical context and the variables biophysical (LEITE et al., 2018a, 2018b; VELOSO; SILVA; FERREIRA, 2020a) above all evapotranspiration (SILVA et al., 2020). However, to understand the relationship between ET and covariable requires robust methods.

Applications of statistical approaches have been growing in the environmental context. For example, models based on multiple linear regressions of the Gaussian family is pointed out as an efficient approach (KARBASI, 2018; BOSQUILIA et al., 2019). The study aimed to analyze ET's behavior by land use and cover and the influence of topographic conditions in time series.

MATERIALS AND METHODS

Study Area

The study area is the Environmental Preservation Area (EPA) of the Pandeiros River, located in the north of Minas Gerais, Brazil, between the coordinate pairs 15° 45' 0" S and 45° 25' W and 14° 55' S and 44° 30' W (DATUM SIRGAS 2000) (Figure 1). The EPA of Pandeiros River is the most extensive in Minas Gerais (3900 km²) and covers the municipalities of Januária, Bonito de Minas, and Cônego Marinho (SANTOS et al., 2020a).

The region's climate is Aw according to the Köppen classification, with colder periods between June and July (and warmer in October), with average (annual) temperature and precipitation of 26 °C and 1057 mm, and high water deficit. (NUNES et al., 2009; SANTOS et al., 2020a). Geomorphology has flat surfaces, depressions, and São Francisco plateaus (SANTOS et al., 2020a), at altitudes between 447 to 859 m. The soils of the region are predominantly Dystrophic Oxisols (UFV; UFLA, 2010). Natural phytophysiognomy has a predominance of Savannas and Low Tree and Shrub Land.

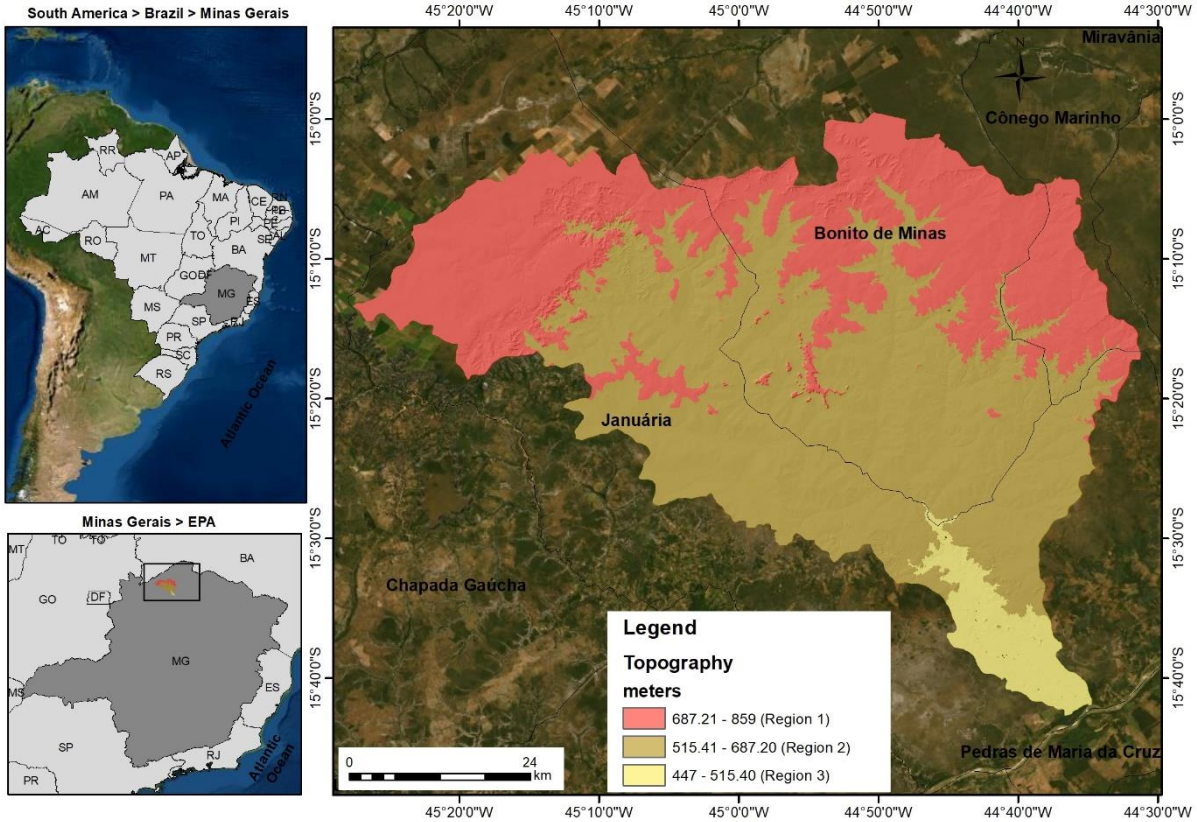

Figure 1 – Location of the Environmental Preservation Area (EPA) on the Pandeiros River, with hypsometric variations highlighted, in Brazil and Minas Gerais.

Data sources and methodological procedures

The methodological framework was divided in five stages: (i) Definition of hypsometric regions based on the altimetric amplitude existing in the EPA of Pandeiros River; (ii) organization of land use and Coverclasses, adapting to the reality of the study area; (iii) ET estimate based on the SAFER model;

(iv) elaboration of a database of spectral and topographic covariable; and (v) Statistical analysis with multiple linear regressions via GLM (Gaussian) between variable and covariables (Figure 2).

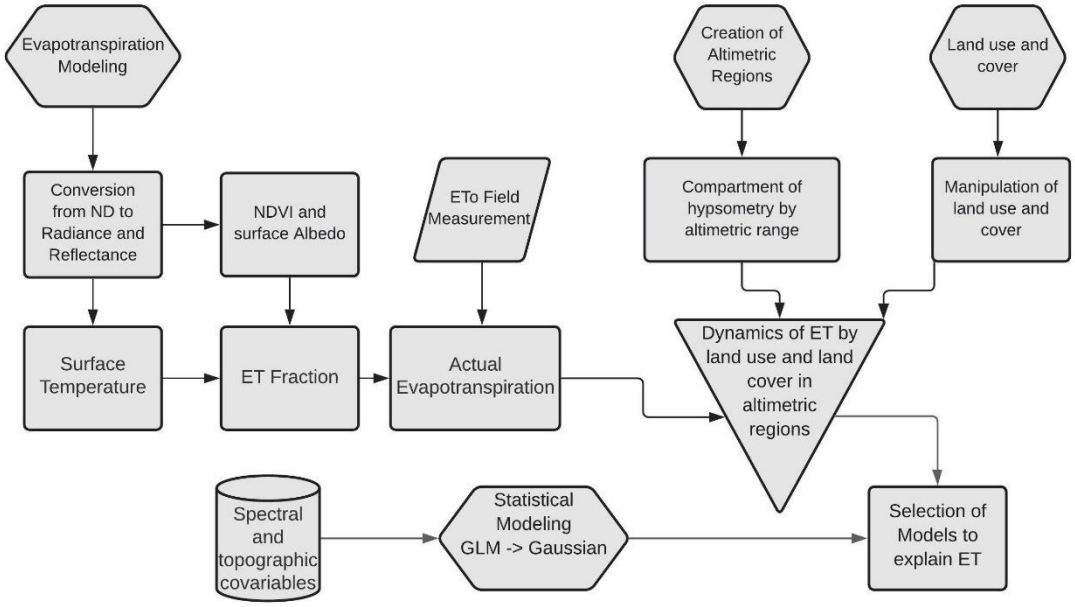

Figure 2 – Flowchart of the processing steps.

Evapotranspiration Modeling

The ET estimation considered images from the Landsat-8 satellite OLI (Operational Terra Imager) and TIRS (Thermal Infrared Sensor) sensors at 30 meters from UMM (Minimum mapping of the unit), with EPA climatic seasonality selection criteria and low cloud cover (dates: 01/21, 02/22, 05/13, and 06/30/2019). The thermal images (TIRS sensor) have 100 meter UMM, so we performed the downscaling to 30 meters, in order to equalize with the OLI sensor images.

January and February represent the rainy season, and May is the beginning of the dry season. The modeling was performed with the SAFER algorithm, which requires the visible, near-infrared, medium, and thermal wavelengths (TEIXEIRA, 2010). The conversion of digital levels to radiance and reflectance was applied using the QGIS software in the images. From this conversion, the Normalized Difference Vegetation Index (NDVI), surface albedo (α), and Surface Temperature (ST) were calculated (SILVA; MANZIONE, 2018). The data (NDVI, α, and ST) were used together with the coefficients a and b (1.8 and -0.008, respectively) to estimate the ratio (ETf) of actual evapotranspiration (ETc) and reference evapotranspiration (ETo) (TEIXEIRA, 2010) (Equation 01).

$$ETf = \exp[a + b\left(\frac{Ts}{\alpha * \mathrm{NDVI}}\right)] \quad \text{(Equation 01)}$$

The ETf is used with an aim similar to the Kc (Crop Coefficient) of FAO (Food and Agriculture Organization) to understand vegetations water needs. ETf is the representation of Kc multiplied by Ks (stress coefficient), which in conditions of absence of stress, Ks would assume a value equal to 1. For these conditions, ETf is similar, or equivalent to Kc. In physical terms, the insertion of NDVI in the calculation is to understand the vegetations vigor, the albedo represented the energy availability of the environment, and the ST shows the humidity status of the environment (VENANCIO et al., 2020). The modeling was done using the R software, raster, rgdal, and water packages (TEAM, 2016).

Based on the ETf and ETo measured at the Januária meteorological station inserted in the study area, the Actual Evapotranspiration (ET) was obtained for each analysis period (Equation 02).

$$ET = ETf \times ETo \quad \text{(Equation 02)}$$

Definition of Altimetric Regions

Evapotranspiration is affected by heterogeneous surface characteristics, including topography (TEIXEIRA et al., 2020). ETo varies according to air temperature (LENKA et al., 2020), directly related to altitude, with a decrease of ~ 0.65 °C every 100 meters (TUBELIS; NASCIMENTO, 1980), based on this premise, in the study area, every 171.8 meters, there is a decrease of ~1 °C in the air temperature. Assuming that air temperature variation occurs concerning altitude, the study area was separated into three altimetric zones using Digital Elevation Model (DEM - SRTM) with 30 m of spatial resolution.

Land Use and Land Cover

The limits and areas of the land use classes derive from the 2018 land use map, with a UMM of 30 meters (MAPBIOMAS, 2018). The main classes are Low Tree and Shrub Land, Annual Culture, Forest, Non-Vegetation, Pasture, Savanna, and Urban. The classes of urban and non-vegetation areas are not present, the first has low expression, and the second is susceptible to regeneration. With prior knowledge of the study area, it was observed that the Palm Swamp Vereda is inserted in forests and savannas, so Palm Swamp Vereda was vectorized with images from WorldView II (50 cm UMM) and were integrated into the mapping.

Database of covariable

The data includes nine prediction covariable (5 spectral and 4 topographic) (Table 1). The spectral products are α (Surface Albedo), EVI2 (Enhanced Vegetation Index), NDBI (Normalized Difference Built-Up Index), MSI (Moisture Stress Index), and surface temperature. Albedo is the ratio of incident and reflected solar radiation, comprising ranges from visible to medium infrared (BONAN, 1997). EVI2 is an improved vegetation index with high sensitivity to variations in biomass in vegetation (JIANG et al., 2008), and phytophysiognomic variety present in the region. The surface temperature was used to show the thermal field for each use and land cover, as the thermal field is influential in the dynamics of evapotranspiration (RAOUFI; BEIGHLEY, 2017). NDBI is typically used to describe the density of areas built in a geographical area (ZHANG; ODEH; HAN, 2009). However, observing its calculation structure, there is a normalization of the medium and near-infrared (XIONG et al., 2012), which can be used to observe variations in vegetation cover. MSI is used to demonstrate the humidity condition in the environments (COHEN, 1991). The indexes were generated using the R software.

Table 1 - Predictor covariable used as input to the model.

Abbreviation	**description**	**Sources**
α	Surface Albedo	Teixeira et al., (2010)
EVI2	Enhanced Vegetation Index 2	Jiang et al., (2008)
NDBI	Normalized Difference Built-Up Index	Zha et al., (2003)
MSI	Moisture Stress Index	Datt e Ravallion (1990)
ST	Surface Temperature	Teixeira et al., (2010)
DEM	Digital Elevation Model	SRTM (2000)
SLOPE	Slope	Evans (1998)
DAH	Diurnal Anisotropic Heating	Böhner e Antonić 2009
TWI	Topographic Wetness Index	Beven and Kirkby (1979)

The topographic products from the SRTM-DEM were: hypsometry, SLOPE, DAH (Diurnal Anisotropic Heating), and TWI (Topographic Wetness Index). These products were generated at SAGA GIS (CONRAD et al., 2015). The hypsometry was used to represent the altimetric variation for each land use because it plays an intrinsic role in wind circulation and water vapor diffusion (MORTENSEN; PETERSEN, 1998). The SLOPE presented in percentage indicates the characteristics of the surface, mainly in terms of its slope. Together with the altitude, the slope is an essential factor in the dynamics of evapotranspiration. The DAH represents heating in different positions of the relief, in the southern hemisphere, faces oriented to the north tend to have higher values of radiation and temperature (CRISTEA et al., 2017). TWI indicates water accumulation potential in the soil, considering the terrain's slope (PETROSELLI et al., 2013). As the work was carried out in a region with a physically varied landscape, this index could explain evapotranspiration.

Statistical Analysis

For statistically sufficient sampling for the EPA area, 10.790 points were distributed following Chuvieco and Huete (2009) recommendations. A minimum spacing of 30 meters between the samples was defined, considering the spatial resolution of the Landsat-8 image, obtaining the land use classes and covariate values per point. Statistical analysis was applied to observe which covariable are most important in explaining ET. The multiple linear regression model GLMs (Generalized Linear Models) of the Gaussian family was considered. It is a process applied in several environmental studies (ROLETT; DIAMOND, 2004; ZEPPETELLO et al., 2020), in which the Gaussian process considers that observations occur in a continuous domain (time or space), each point in space is associated with a random variable with a normal distribution (REYNOLDS, 2009). These premises are suitable for the study due to the sample distribution of points in the region. A complete model was built with the nine predictor variables (Equation 3) for each use and land cover in altimetric areas.

$$\boldsymbol{Model} < - glm(ET \sim \alpha + EVI2 + ST + NDBI + DAH + SLOPE + MDE + TWI + MSI, family = gaussian) \quad \text{(Equation 3)}$$

The beckward function was applied to eliminate non-significant variables with the AKAIKE (AIC) criteria (NAIK; SHI; TSAI, 2007). The model's efficiency test considered the effect of multicollinearity between covariable using the VIF (Variance Inflation Factor) function. In the initial model, covariable with VIF > 5 was removed, forming a new model, with repetition in the search for the ideal model with all covariates with VIF <5 (YU; JIANG; LAND, 2015). Excellent models were obtained for each use and land cover analyzed after this application, totaling 60 models.

RESULTS

Land Use and Cover by Altimetric Region

In general, there is a predominance of Savannas (arboreal and shrub-herbaceous strata) in all regions. The Low Tree and Shrub Land, and Forest formations predominate in the A1 altimetric region, with 65, 21, and 7% of the areas, respectively (Figure 3). In the west region, there is a concentration of Annual Crops (~ 3%). The pasture has a spatial distribution pattern, with proximity to forests, especially those bordering water bodies, similar to previous studies in EPA (DIAS; MOSCHINI; TREVISAN, 2017). In the A2 region, the Savannas class (~ 50%, 15% less than region A1) predominates, followed by the Low Tree and Shrub Land (16% higher than region A1) and Pastures with 37% and 5%, respectively. Most of the Palm Swamp Veredas are concentrated in this region, with ~64.30 km^2 (51.35 km² or 78.86% higher than in the A1 region). In the A3 region, Savannas occupy the largest share (59%), followed by Pastures and Forests, both with ~ 17%.

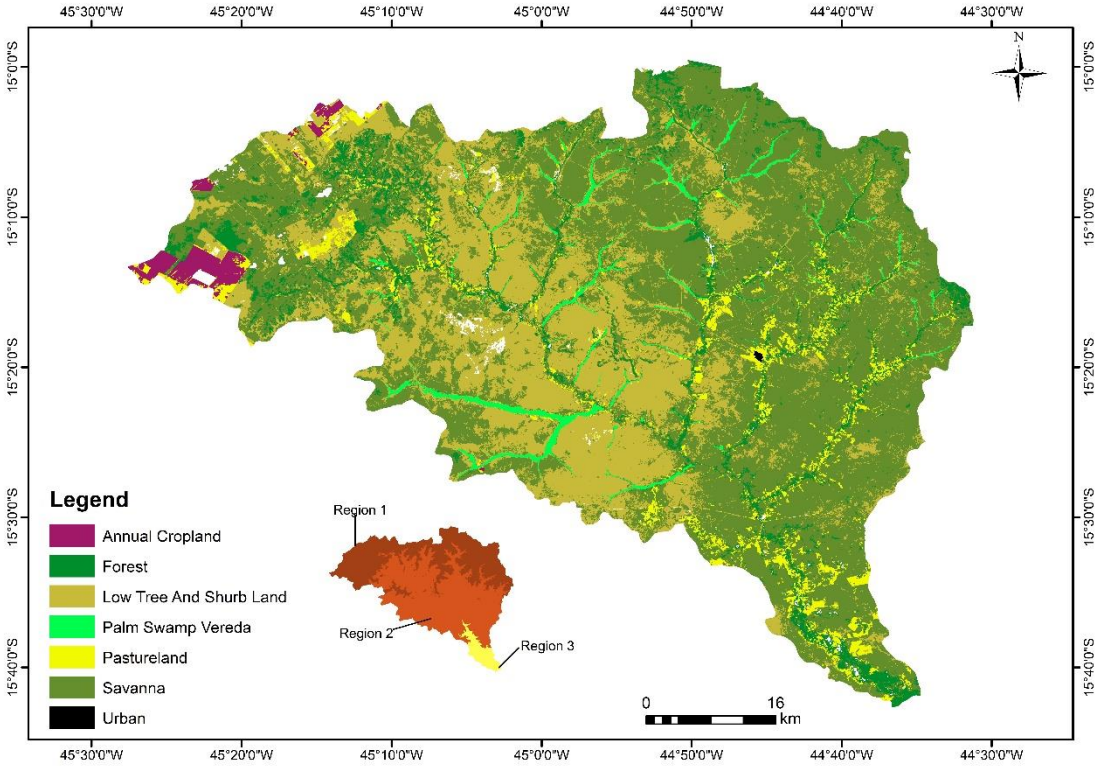

Figure 3 - Spatial distribution of land use and Cover in the Pandeiros River EPA, Minas Gerais.

Spatio-temporal distribution of ET

The wetter period represents higher rates of ET. In this period, the amplitude is 10.24 mm d^{-1}. The highest values occur in the areas bounded by forests (Figure 4). Even in the dry season (with water restriction), these areas have the highest ET values (2.6 to 7.89 mm d^{-1}). For all periods, there is a trend of lower ET values (0 to 1.25 mm d^{-1}) occurring in the central, western, and northern portions of the EPA, areas with a predominance of Low Tree and Shrub Land. The other extensions of the EPA intermediate values were predominant (0.85 to 3.07 mm d^{-1}), mainly due to the Cerrado areas spatiality.

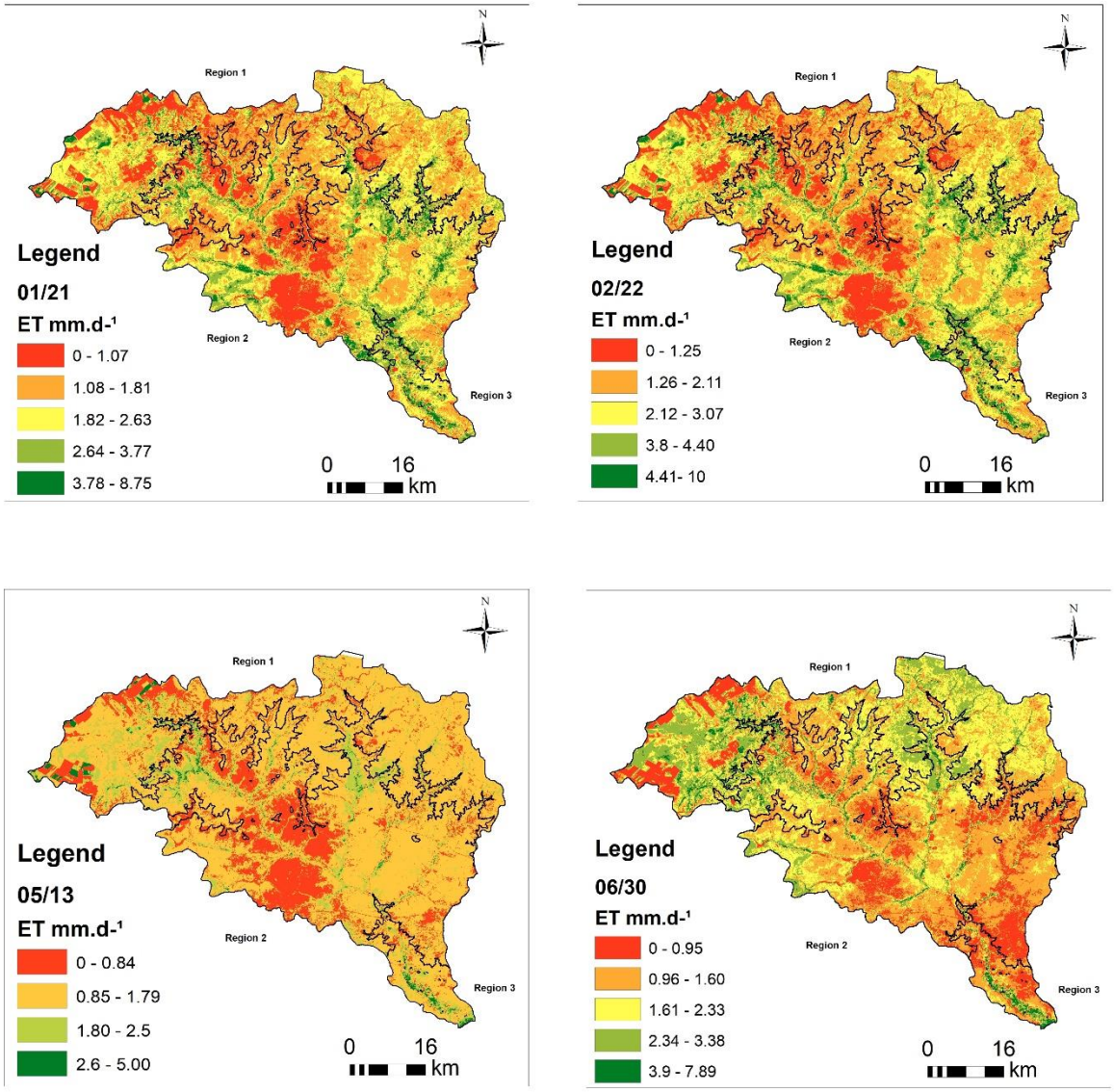

Figure 4 - Spatio-temporal distribution of ET at the Pandeiros River EPA on 01/21, 02/22, 05/13, and 06/30 2019.

The average ET values for the A1 region for 01/21, 02/22, 05/13, and 06/30 were 1.71, 2.00, 1.22, and 1.84 mm d^{-1}, respectively. In the A2 region, the average values were 1.93, 2.26, 1.15, and 1.52 mm d^{-1}, for 01/21, 02/22, 05/13, and 06/30, respectively. For region 3, ET averages 01/21, 02/22, 05/13, and 06/30 were 2.40, 2.80, 1.44, and 1.51 mm d^{-1}, respectively. The highest ET values were defined for the Forest areas. In general, the ET means of region 3 is higher than the other regions (1 and 2).

Covariables Selected to Explain ET by GLM (Gaussian) Model

The methodology created 60 models for each covariate (nine), and the low Akaike criterion is the best model (ASPINALL, 2004). All covariables in the database were related to some of the models (Table 2). The spectral and topographic matrix covariable were efficient in the model combinations in all altimetric regions.

Table 1 - Models selected by land use and land cover in regions 1, 2, and 3, for the periods from 01/21, 02/22, 05/13, and 06/30 in the EPA of Pandeiros River.

		REGION A1		
LU/LC	**01/21**	**02/22**	**05/13**	**06/30**

Low Tree and Shrub Cerrado	α, ST, DAH, MDE	α, DAH, MDE	α, ST, MDE	α, EVI2, ST, DAH, MDE
Annual Croplands	α	α	α, EVI2	α, ST
Forest	MDE	ST, DAH, SLOPE	α, ST, EVI2, DAH	α, ST, SLOPE
Pastureland	ST	α, EVI2, MDE, TWI	ST, TWI	ST
Savanna	EVI2, ST, MSI	α, EVI2, ST	α, EVI2, ST	α, ST
Palm Swamp Veredas	ST, SLOPE	ST	α, ST, DAH, MDE, TWI	α, EVI2, ST, TWI
		REGION A2		
LU/LC	**01/21**	**02/22**	**05/13**	**06/30**
Low Tree and Shrub Cerrado	EVI2, ST	α, EVI2, ST	α, EVI2, ST, NDBI	α, EVI2, ST
Forest	α, ST	α, EVI2, ST, MSI	α, EVI2, ST, MDE	EVI2, ST, MDE
Pastureland	α, EVI2, ST	α, ST, MDE, TWI	ST, DAH, MDE	α, ST
Savanna	α, ST, DAH	α, EVI2, ST, DAH, SLOPE	α, EVI2, ST, DA, MDE	α, ST, DAH, SLOPE, MDE
Palm Swamp Veredas	ST, MDE	α, ST, MDE	ST, TWI	ST, DAH, MDE
		REGION A3		
LU/LC	**01/21**	**02/22**	**05/13**	**06/30**
Low Tree and Shrub Cerrado	α, NDBI, MSI	EVI2, ST, MDE	EVI2, ST, MDE	ST, MDE
Pastureland	ST, TWI	ST	ST, MDE	α, ST
Forest	α, ST	α, EVI2, ST, NDBI, MDE	α, EVI2, NDBI, MDE, TWI	EVI2, ST
Savanna	ST, MDE	ST, MDE	α, EVI2, ST	α, ST, DAH

Source: Landsat 8 and SRTM. ST: Surface Temperature, α: Surface Albedo, EVI2: Enhanced Vegetation Index 2, MSI: Moisture Stress Index (Landsat Dataset), Slope, MDE: Digital Elevation Model, DAH: Diurnal Anisotropic Heating, TWI: Topographic Wetness Index (SRTM Dataset).

Evapotranspiration by Land Use and Cover by Altimetric Regions

In region A1, the wet period corresponding to January and February in 2019, the highest ET rates occurred in Forests, while the lowest was in Low Shrub and Land areas (Figure 5). This pattern was maintained in the dry period (05/13). In the following month (06/30), the lowest rate of ET was in areas of Annual Crops, while Forests have a high standard of ET.

In all periods in the A2 region, the highest ET values occurred in the Forest areas (Figure 5); on the other hand, the Low Tree and Shrub Land have the lowest ET values during most of the period. In region A3, following the trend of other altimetric regions, forests have higher rates of ET (Figure 5). For the periods from 01/21, 02/22, and 05/13, the lowest values occurred in the areas of Low Tree and Shrub Land. Although this trend occurs, in region A3, on 06/30, the lowest rate of ET was registered in Pastures. In the general trend for land uses and land cover in the regions, ET values peak on 02/22, with a steep decline on 05/13.

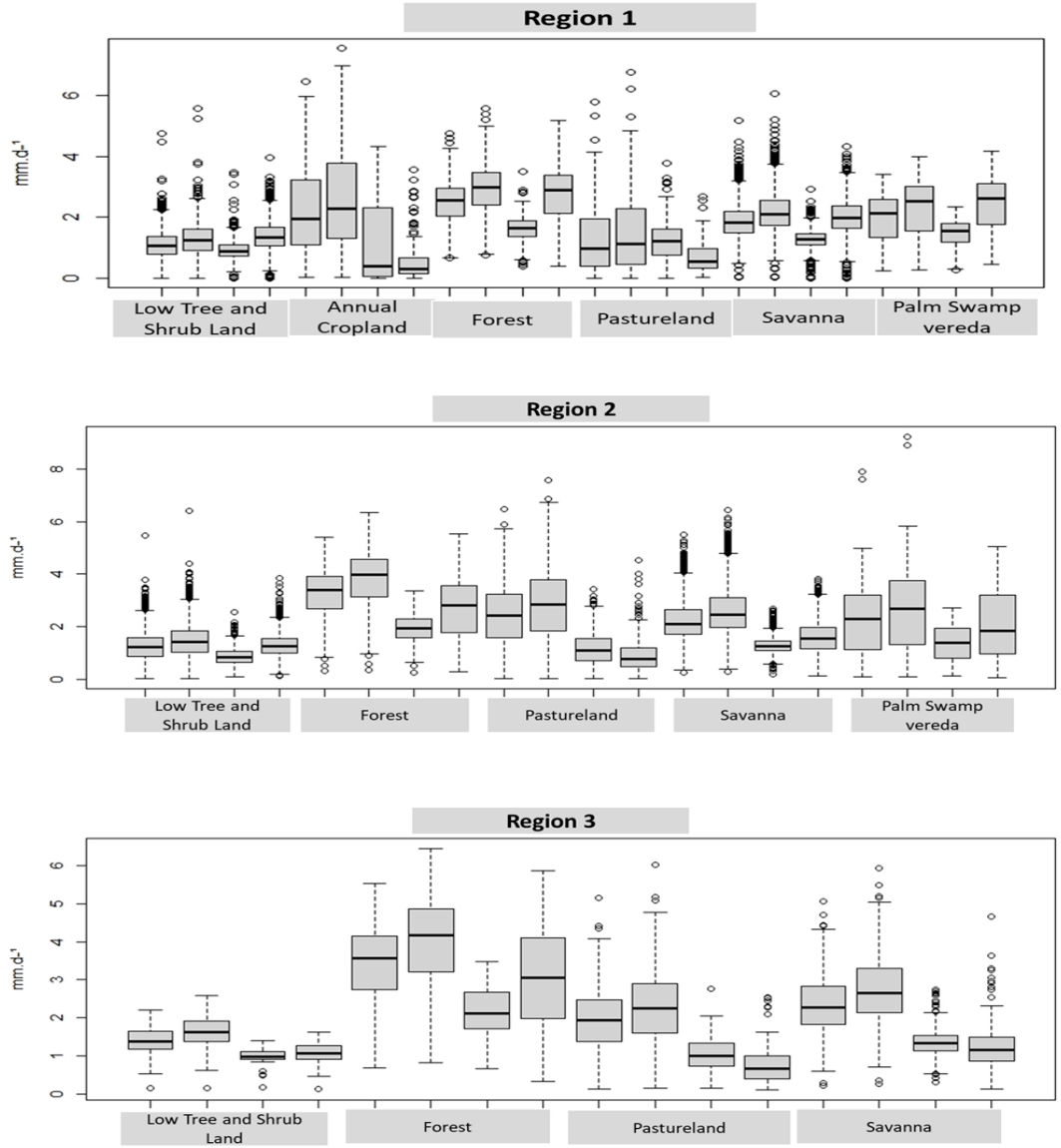

Figure 5 - Evapotranspiration by land use and cover, and Altimetric Regions, in the periods from 01/21, 02/22, 05/13 and 06/30 2019.

The classes of land use and cover in region A3 (with lower altimetric levels) showed higher ET values than the other regions in most of the periods analyzed (Figure 6).

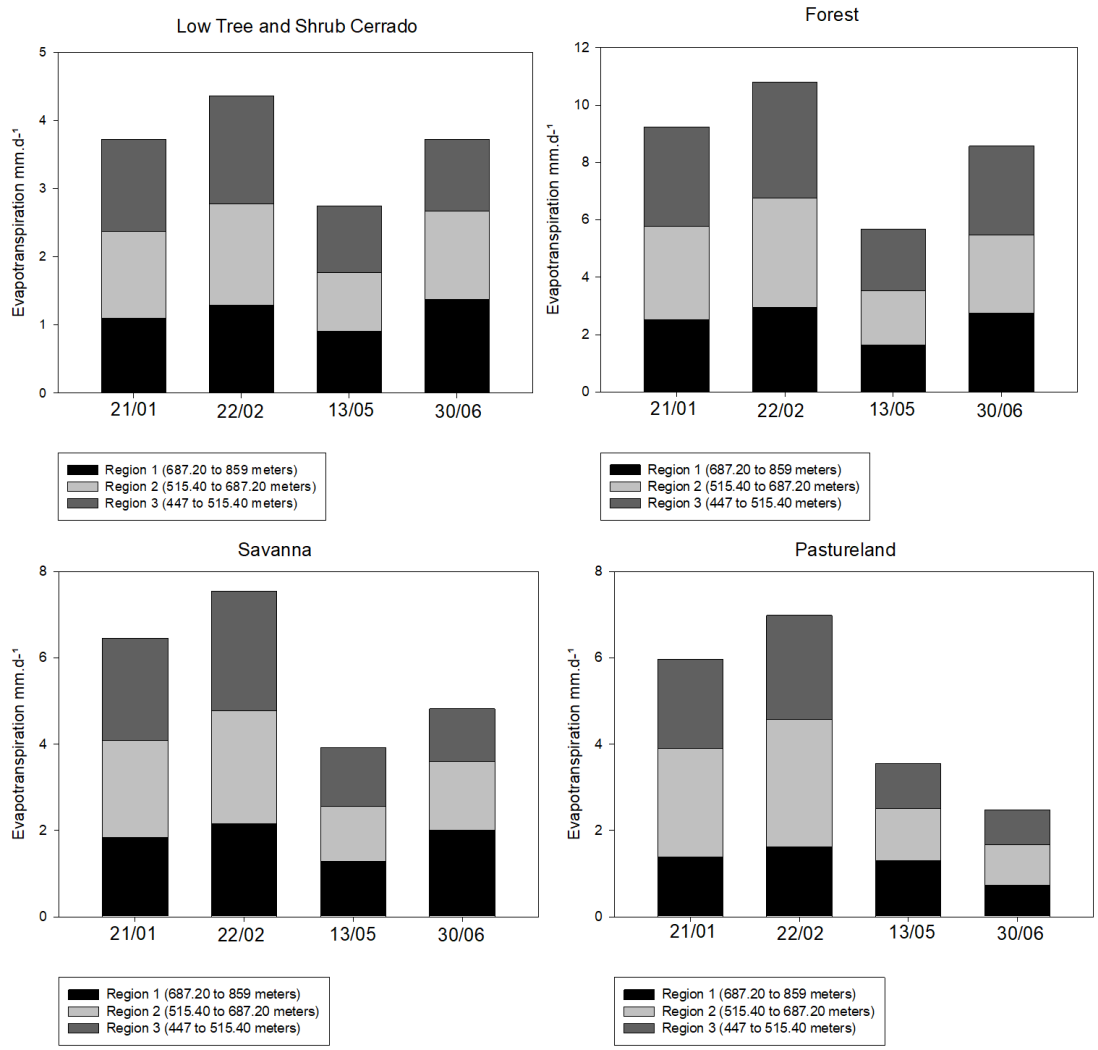

Figure 6 - Evapotranspiration of Land Uses and Cover in Altimetric Regions 1, 2, and 3, on 01/21, 02/22, 05/13, and 06/30, at the Rio Pandeiros EPA.

DISCUSSION

Relationship between ET and covariables of land use and land cover

The altimetric condition as a climatic condition did not influence ET rates. But how the landscape layout influenced it, especially providing the highest ET rates for the areas with the lowest altimetric levels (region 3). Region 3 comprises a swampy environment, with high water availability in the soil, due to the water table's proximity to the soil surface. This influence is evident when observing the predominance of topographic indices in explaining the ET for this region, mainly the TWI (Table 2), an aspect that influences ET in the study area (VELOSO; SILVA; FERREIRA, 2020a). This water availability promotes the supply of the physiological needs of vegetation, maintaining the highest ET levels compared to other regions, in which sandy soils are predominant (NUNES et al., 2009) and with low water availability.

Regarding land use, in the Low Tree and Shrub Land, the ET rate was low (regions A1 and A3), and spectral covariable was predominant in the models. The most relevant spectral covariables were albedo and ST, as they are part of the SAFER algorithm (TEIXEIRA, 2010). In this class, the ST and Alb present high values due to the phenological design, with short stature and discontinuous canopies, maintaining soil exposure and rocky material (EITEN, 1972). Therefore, incident solar radiation overheats the surface, intensifying the sensible heat exchange between the soil surface and the air layers (LOPES; SILVA; PENHA PACHECO, 2014). Nevertheless, these areas play a crucial role in the climate context despite the low ET. Simultaneously, short-wave radiation is reflected with greater intensity, increasing the reflection coefficient, making these open environments key in energy dynamics as they release energy from the system (VELDMAN et al., 2019).

The topographic covariables, DEM and slope were more significant to explain ET variation in forests. This aspect is related to the arrangement of forests in the landscape. Riparian forests occurred in flat environments, with proximity to water bodies, easy access to underground water, and high evapotranspiration dynamics even in dry periods. The closed and continuous canopy enables more extensive interception of solar radiation and conversion to latent heat fluxes (CIRELLI; PENTEADO-DIAS, 2003), providing a high ET rate.

Forests class also involves dry forests, which develop in sloping environments, under Karst relief areas (MELO et al., 2013), and this physical characteristic infers the phenological dynamics of the vegetation. In dry periods, there is a loss of ~ 95% of the leaves (FONSECA et al., 2018), moderating the exchange of energy with the atmosphere (RANKINE et al., 2017) and ET rates (VELOSO; FERREIRA; SILVA, 2017); therefore, the dry forest is an essential phytophysiognomy for water management in a region. They avoid excessive water loss, maintaining water availability in the soils deepest layers, being necessary for environmental management plans.

The spectral covariable (ST and EVI2) also contributed to explaining ET variation in the forest domain. In wet periods, EVI2 values in the Forest class are high (JIANG et al., 2008), which decreases albedo and ST, and increases energy availability for the vegetation's metabolic processes, especially evapotranspiration. In dry periods, with a decreasing trend of EVI2 (NEVES et al., 2016), there is a significant loss of energy by albedo, keeping less energy available, and the remaining balance on the surface is used for heating the air due soil moisture conditions (LARSON et al., 2009).

In Savannas, ST, Albedo, EVI2, and MSI explained ET. The temperatures in these environments are usually high, depending on vegetation characteristics (herbaceous and deciduous, spaced) (SANTOS; FERREIRA; FERREIRA, 2011) allowing the direct incidence of solar radiation on the soil matrix, causing the diffusion of sensitive heat to heat the air. These characteristics also lead to more significant energy losses due to albedo, especially forested areas, which tend to decrease ET rates.

EVI2, in these environments, tends to be higher in the wetter periods, providing an increase in the ET rate and lower dry periods (NEVES et al., 2016). The MSI stood out in the wetter period (02/22), related to rain occurrence. This index reflects soil moisture conditions, as it comprises vegetation stress (COHEN, 1991), a latent heat flow diffusion controller (LEI et al., 2018), responsible for the high rates of ET. The DEM and the slope for these areas represent their position in the landscape, as in the other classes. In most cases, the DAH in the Savannas areas was equal to zero, indicating no daytime heating and maintaining the ET rates.

In Palm Swamp Veredas, there was a predominance of topographic variables (DEM, SLOPE, DAH, and TWI). Palm Swamp Veredas occur in flat areas, influenced by the Groundwater confined by low permeability rocks (ALENCAR-SILVA; MAILLARD, 2011), a factor that determines the soil moisture demand in these environments for most of the year. Veloso, Silva, and Ferreira (2020) analyzed the energy balance in Palm Swamp Veredas at EPA Pandeiros River and found a relationship between the ET and TWI rates, corroborating our results.

From the spectral covariables, ST and Albedo were the predominant ones in explaining ET for Palm Swamp Veredas. ST and albedo maintain low values compared to other types of vegetation in the Cerrado (VELOSO; SILVA; FERREIRA, 2020b), providing high ET (SILVA et al., 2020). Palm Swamp Veredas have discontinuous canopies, facilitating the circulation of winds and increasing water vapor flows. These areas play an essential role in the Brazilian Cerrado region, as they are genetic banks of animal species, have a rich flora, supply water bodies in the biome.

Among anthropic use classes, such as Annual Croplands the ET was explained predominantly by spectral covariables (albedo, ST, and EVI2). In the rainy periods (01/21 to 02/22), crop production increases, favoring the interception and absorption of incident solar radiation and reducing the loss of surface energy by albedo (SANTOS et al., 2017). In the rainy periods ~80% of the absorbed energy is converted into sensitive heat flow flows (BEZERRA et al., 2014).

The ET variation influences the plants phenological cycle, with ET rates decreasing sharply in less rainfall (between 05/13 and 06/30), and EVI2 represents this dynamic. The biomass in these environments tends to decrease (ALAM; LAMB; RAHMAN, 2018) due to scarce water availability and harvest period, which leads to lower ET rates (RUHOFF et al., 2012). In this period, the albedo was an explanatory variable of ET, with an inverse role compared to wet periods (01/21 and 02/22), which is associated with a decrease in the senescence period ET rates (MUSSI et al., 2020b). Senescence also influences ST, keeping its values high (CAIONI et al., 2020) and decreasing ET rates. Annual Croplands are essential for the regions economic context. Still, considering the behavior of ET, conversions of natural areas for this class increases surface temperature (SILVÉRIO et al., 2015), because of excessive

loss of energy through albedo (COSTA et al., 2007), sharp drops in ET rates (LATHUILLIÈRE et al., 2018) and humidity of the adjacent atmospheric layers (QIU et al., 2011).

In the Pasture areas, ST, Albedo, and in the topographic indices, TWI and DEM predominated to explain ET. In rainy periods, pastures have high biomass levels (VELOSO et al., 2020); this is associated with their direct contact with the water in the soil layers. When the incidence of radiation is considered constant in these environments, there is a decrease in the reflection coefficient (SILVA; MANZIONE, 2018). With low albedo values and high biomass levels, surface radiation is used more efficiently in transferring water to the atmosphere through ET (SILVA et al., 2020). ST for these areas is high (CAIONI et al., 2020), inferring ET dynamics (with a decrease). As in the other classes, the DEM represents the position of use of the landscape. The pastures are concentrated in low altimetric levels and flat relief, which provides water availability, mainly considering that the TWI is among the explanatory variables.

From a seasonal point of view, there is a decrease in ET rates in dry periods in pastures, with a tendency for pasture areas (BRITO et al., 2018; VELOSO et al., 2020). Pastures in the general context of livestock play an essential role in the Brazilian economy, representing 31% of Gross Domestic Product (GDP), placing Brazil the second-largest meat exporter in the world (VELOSO et al., 2020). However, studies show that pastureland has some degree of degradation (PEREIRA et al., 2018), which changes the hydrothermal dynamics of a region, mainly resulting in a decrease in ET rates (ANDRADE et al., 2016) and water availability in the soil.

As can be seen, evapotranspiration obtained a particular variation for each use and land cover under different altimetric conditions, being explained by spectral and topographic variables in the Pandeiros River EPA.

Conclusions

Evapotranspiration for the study area showed seasonal patterns, with the highest values occurring in the rainy season (02/22) and the lowest values in the dry season (05/13) of 2019. Among the land uses, Forests have the highest ET values for all topographic regions, being a vital climate controller, moistening the surface, and transferring the latent heat to the adjacent atmosphere.

Spectral and topographic sets were useful in explaining evapotranspiration using multiple GLM (Gaussian) regressions. With the selection of covariables consistent with the literature for all uses and land cover.

Intrinsic characteristics of the study area, such as the Pantanal environment in region 3 or the presence of wetlands, both with greater availability have high rates of ET in dry and wet periods.

REFERENCES

AB'SABER, A. N. Províncias geológicas e domínios morfoclimáticos no Brasil. **Geomorfologia PP - São Paulo**, n. 20, p. 1–26, 1970.

ALAM, M. S.; LAMB, D. W.; RAHMAN, M. M. A refined method for rapidly determining the relationship between canopy NDVI and the pasture evapotranspiration coefficient. **Computers and Electronics in Agriculture**, v. 147, p. 12–17, 2018.

ALENCAR-SILVA, T.; MAILLARD, P. Delimitação, caracterização e tipologia das veredas do Parque Estadual Veredas do Peruaçu. **Revista Geografias**, p. 24–39, 2011.

ALTHOFF, D. et al. Evapotranspiration for irrigated agriculture using orbital satellites. **Bioscience Journal**, v. 35, n. 3, 2019.

ANDERSON, M. C. et al. Use of Landsat thermal imagery in monitoring evapotranspiration and managing water resources. **Remote Sensing of Environment**, v. 122, p. 50–65, 2012.

ANDRADE, R. G. et al. Analysis of evapotranspiration and biomass in pastures with degradation indicatives in the Upper Tocantins River Basin, in Brazilian Savanna. **Revista Ceres**, v. 63, n. 6, p. 754–760, 2016.

ARANTES, A. E.; FERREIRA, L. G.; COE, M. T. The seasonal carbon and water balances of the Cerrado environment of Brazil: Past, present, and future influences of land cover and land use. **ISPRS Journal of Photogrammetry and Remote Sensing**, v. 117, p. 66–78, 2016.

BEZERRA, J. M. et al. Parâmetros biofísicos obtidos por sensoriamento remoto em região semiárida do

estado do Rio Grande do Norte, Brasil. **Revista Brasileira de Engenharia Agrícola e Ambiental**, v. 18, n. 1, p. 73–84, 2014.
BONAN, G. B. Effects of land use on the climate of the United States. **Climatic Change**, v. 37, n. 3, p. 449–486, 1997.
BOSQUILIA, R. W. D. et al. Evaluation of evapotranspiration variations according to soil type using multivariate statistical analysis. **Geoderma**, v. 355, p. 113906, 2019.
BRITO, J. L. S. et al. MODIS estimates of pasture productivity in the Cerrado based on ground and Landsat-8 data extrapolations. **Journal of Applied Remote Sensing**, v. 12, n. 2, p. 26006, 2018.
CAIONI, C. et al. Droughts amplify differences between the energy balance components of Amazon forests and croplands. **Remote Sensing**, v. 12, n. 3, p. 525, 2020.
CASTRO TEIXEIRA, A. H. et al. Modeling large-scale biometeorological indices to monitor agricultural-growing areas: applications in the fruit circuit region, São Paulo, Brazil. **International Journal of Biometeorology**, p. 1–12, 2020.
CIRELLI, K. R. N.; PENTEADO-DIAS, A. M. Análise da riqueza da fauna de Braconidae (Hymenoptera, Ichneumonoidea) em remanescentes naturais da Área de Proteção Ambiental (APA) de Descalvado, SP. **Revista Brasileira de Entomologia**, v. 47, n. 1, p. 89–98, 2003.
COHEN, W. Response of vegetation indices to changes in three measures of leaf water stress. **Photogrammetric Engineering and Remote Sensing**, v. 57, n. 2, p. 195–202, 1991.
CONRAD, O. et al. System for automated geoscientific analyses (SAGA) v. 2.1. 4. **Geoscientific Model Development Discussions**, v. 8, n. 2, 2015.
COSTA, M. H. et al. Climate change in Amazonia caused by soybean cropland expansion, as compared to caused by pastureland expansion. **Geophysical Research Letters**, v. 34, n. 7, p. 1–4, 2007.
CRISTEA, N. C. et al. An evaluation of terrain-based downscaling of fractional snow covered area data sets based on LiDAR-derived snow data and orthoimagery. **Water Resources Research**, v. 53, n. 8, p. 6802–6820, 2017.
DIAS, L. C. C.; MOSCHINI, L. E.; TREVISAN, D. P. A Influência das Atividades Antrópicas na Paisagem da Área de Proteção Ambiental Estadual do Rio Pandeiros, MG-Brasil. **Fronteiras: Journal of Social, Technological and Environmental Science**, v. 6, n. 2, p. 85–105, 2017.
EITEN, G. The cerrado vegetation of Brazil. **The Botanical Review**, v. 38, n. 2, p. 201–341, 1972.
FERREIRA, L. B. et al. Estimation of reference evapotranspiration in Brazil with limited meteorological data using ANN and SVM–A new approach. **Journal of hydrology**, v. 572, p. 556–570, 2019.
FONSECA, M. B. et al. Leaf damage and functional traits along a successional gradient in Brazilian tropical dry forests. **Plant ecology**, v. 219, n. 4, p. 403–415, 2018.
HEMAKUMARA, H. M.; CHANDRAPALA, L.; MOENE, A. F. Evapotranspiration fluxes over mixed vegetation areas measured from large aperture scintillometer. **Agricultural water management**, v. 58, n. 2, p. 109–122, 2003.
IMMERZEEL, W. W.; DROOGERS, P. Calibration of a distributed hydrological model based on satellite evapotranspiration. **Journal of hydrology**, v. 349, n. 3–4, p. 411–424, 2008.
JIANG, Z. et al. Development of a two-band enhanced vegetation index without a blue band. **Remote sensing of Environment**, v. 112, n. 10, p. 3833–3845, 2008.
KIPTALA, J. K. et al. Mapping evapotranspiration trends using MODIS and SEBAL model in a data scarce and heterogeneous landscape in Eastern Africa. **Water resources research**, v. 49, n. 12, p. 8495–8510, 2013.
LARSON, K. M. et al. GPS multipath and its relation to near-surface soil moisture content. **IEEE Journal of Selected Topics in Applied Earth Observations and Remote Sensing**, v. 3, n. 1, p. 91–99, 2009.
LATHUILLIÈRE, M. J. et al. Rain-fed and irrigated cropland-atmosphere water fluxes and their implications for agricultural production in Southern Amazonia. **Agricultural and Forest Meteorology**, v. 256, p. 407–419, 2018.
LEI, F. et al. Global investigation of soil moisture and latent heat flux coupling strength. **Water resources research**, v. 54, n. 10, p. 8196–8215, 2018.
LEITE, M. E. et al. Análise do Comportamento do Saldo de Radiação Instantâneo em Áreas de Cerrado por Produtos Orbitais (Analyze of Behavior of Net Radiation Instantaneous in the Areas of Cerrado by Orbitals Products). **Revista Brasileira de Geografia Física**, v. 11, n. 6, p. 2067–2080, 2018a.
LEITE, M. E. et al. Geotecnologias aplicadas a estimativa da temperatura de superfície em diferentes usos e ocupações do solo na Área de Proteção Ambiental do Rio Pandeiros–Minas Gerais/Geotechnologies applied to the surface temperature estimation in different soil uses and .

Caderno de Geografia, v. 28, n. 53, p. 490–509, 2018b.
LENKA, N. K. et al. Carbon dioxide and temperature elevation effects on crop evapotranspiration and water use efficiency in soybean as affected by different nitrogen levels. **Agricultural Water Management**, v. 230, p. 105936, 2020.
LOPES, H. L.; SILVA, B. B.; PENHA PACHECO, A. Distribuição espacial do saldo de radiação e do fluxo de calor no solo no território de Itaparica, Nordeste do Brasil. **Revista Brasileira de Cartografia**, v. 66, n. 2, 2014.
MARX, A. et al. Uncertainty analysis for satellite derived sensible heat fluxes and scintillometer measurements over Savannah environment and comparison to mesoscale meteorological simulation results. **Agricultural and Forest Meteorology**, v. 148, n. 4, p. 656–667, 2008.
MELESSE, A. M. et al. Remote sensing sensors and applications in environmental resources mapping and modelling. **Sensors**, v. 7, n. 12, p. 3209–3241, 2007.
MELO, P. H. A. DE et al. Composição florística de angiospermas no carste do alto São Francisco, Minas Gerais, Brasil. **Rodriguésia**, v. 64, n. 1, p. 29–36, 2013.
MORTENSEN, N. G.; PETERSEN, E. L. **Influence of topographical input data on the accuracy of wind flow modelling in complex terrain**. 1997 European Wind Energy Conference. **Anais**...Irish Wind Energy Association, 1998
MUSSI, R. F. et al. Sugarcane evapotranspiration estimated by safer algorithm for evapotranspiration retrieving. **IRRIGA**, v. 25, n. 2, p. 263–278, 2020a.
MUSSI, R. F. et al. EVAPOTRANSPIRAÇÃO DA CANA-DE-AÇÚCAR ESTIMADA PELO ALGORITMO SAFER. **IRRIGA**, v. 25, n. 2, p. 263–278, 2020b.
NAIK, P. A.; SHI, P.; TSAI, C.-L. Extending the Akaike information criterion to mixture regression models. **Journal of the American Statistical Association**, v. 102, n. 477, p. 244–254, 2007.
NEVES, A. K. et al. Combining time series features and data mining to detect land cover patterns: a case study in northern Mato Grosso state, Brazil. **Revista Brasileira de Cartografia**, v. 68, n. 6, p. 1–10, 2016.
NUNES, Y. R. F. et al. Pandeiros: o pantanal mineiro. **MG Biota**, v. 2, n. 2, p. 4–17, 2009.
PEREIRA, O. J. R. et al. Assessing Pasture Degradation in the Brazilian Cerrado Based on the Analysis of MODIS NDVI Time-Series. **Remote Sensing**, v. 10, n. 11, p. 1–14, 2018.
PETROSELLI, A. et al. Ecological behavior of Quercus suber and Quercus ilex inferred by topographic wetness index (TWI). **Trees**, v. 27, n. 5, p. 1201–1215, 2013.
PÔÇAS, I. et al. Using remote sensing energy balance and evapotranspiration to characterize montane landscape vegetation with focus on grass and pasture lands. **International Journal of Applied Earth Observation and Geoinformation**, v. 21, p. 159–172, 2013.
QIU, G. Y. et al. Effects of the "Conversion of Cropland to Forest and Grassland Program" on the water budget of the Jinghe River catchment in China. **Journal of Environmental Quality**, v. 40, n. 6, p. 1745–1755, 2011.
RANKINE, C. et al. Comparing MODIS and near-surface vegetation indexes for monitoring tropical dry forest phenology along a successional gradient using optical phenology towers. **Environmental Research Letters**, v. 12, n. 10, p. 105007, 2017.
RAOUFI, R.; BEIGHLEY, E. Estimating daily global evapotranspiration using penman–monteith equation and remotely sensed land surface temperature. **Remote Sensing**, v. 9, n. 11, p. 1138, 2017.
REYNOLDS, D. A. Gaussian Mixture Models. **Encyclopedia of biometrics**, v. 741, 2009.
ROLETT, B.; DIAMOND, J. Environmental predictors of pre-European deforestation on Pacific islands. **Nature**, v. 431, n. 7007, p. 443–446, 2004.
RUHOFF, A. L. et al. A MODIS-based energy balance to estimate evapotranspiration for clear-sky days in Brazilian tropical savannas. **Remote Sensing**, v. 4, n. 3, p. 703–725, 2012.
RUHOFF, A. L. et al. Assessment of the MODIS global evapotranspiration algorithm using eddy covariance measurements and hydrological modelling in the Rio Grande basin. **Hydrological Sciences Journal**, v. 58, n. 8, p. 1658–1676, 2013.
SACKS, W. J.; KUCHARIK, C. J. Crop management and phenology trends in the US Corn Belt: Impacts on yields, evapotranspiration and energy balance. **Agricultural and Forest Meteorology**, v. 151, n. 7, p. 882–894, 2011.
SANTOS, C. A. G. et al. Estimation of evapotranspiration for different land covers in a Brazilian semi-arid region: A case study of the Brígida River basin, Brazil. **Journal of South American Earth Sciences**, v. 74, p. 54–66, 2017.
SANTOS, N. B. F. DOS; FERREIRA, L. G.; FERREIRA, N. C. Análise espacial da temperatura de

superfície no cerrado: uma análise sazonal a partir de dados orbitais de resolução moderada, para o período de 2003 a 2008. **Cienc. Cult.**, v. 63, p. 30–33, 2011.
SANTOS, G. L. et al. Anthropogenic and climatic influences in the swamp environment of the Pandeiros River basin, Minas Gerais-Brazil. **Environmental Monitoring and Assessment**, v. 192, n. 4, p. 1–11, 2020a.
SANTOS, J. E. O. et al. Performance of SAFER evapotranspiration using missing meteorological data. **Agricultural Water Management**, v. 233, p. 106076, 2020b.
SCHERER-WARREN, M. Desmembramento de estimativas de evapotranspiração obtidas por sensoriamento remoto nas componentes de evaporação e transpiração vegetal. **Rev Bras Geogr Fısica**, p. 361–373, 2012.
SENAY, G. B. Modeling landscape evapotranspiration by integrating land surface phenology and a water balance algorithm. **Algorithms**, v. 1, n. 2, p. 52–68, 2008.
SILVA, C. DE O. F.; CASTRO TEIXEIRA, A. H.; MANZIONE, R. L. Agriwater: An R package for spatial modelling of energy balance and actual evapotranspiration using satellite images and agrometeorological data. **Environmental Modelling & Software**, v. 120, p. 104497, 2019.
SILVA, C. DE O. F.; MANZIONE, R. L. MODELAGEM ESPACIAL DA EVAPOTRANSPIRAÇÃO EM AGROECOSSISTEMA DO SISTEMA AQUÍFERO BAURU. **Águas Subterrâneas**, 2018.
SILVA, L. A. P. DA et al. Estimating Water Loss in an Environmental Protection Area - Minas Gerais, Southeast Brazil. **Caderno de Geografia**, v. 30, n. 62, p. 1–20, 2020.
SILVA, L. C. L. et al. Pedodiversidade no estado de Minas Gerais-Brasil. **Caderno de Geografia**, v. 28, n. 1, p. 18–38, 2018.
SILVÉRIO, D. V et al. Agricultural expansion dominates climate changes in southeastern Amazonia: the overlooked non-GHG forcing. **Environmental Research Letters**, v. 10, n. 10, p. 104015, 2015.
SOUZA, C. M. P. DE et al. Multivariate Analysis and Machine Learning in Properties of Ultisols (Argissolos) of Brazilian Amazon. **Revista Brasileira de Ciência do Solo**, v. 42, 2018.
TEAM, R. C. R Foundation for Statistical Computing. R: A language and environment for statistical computing. **Vienna, Austria**, 2016.
TEIXEIRA, A. H. DE C. Determining regional actual evapotranspiration of irrigated crops and natural vegetation in the São Francisco river basin (Brazil) using remote sensing and Penman-Monteith equation. **Remote Sensing**, v. 2, n. 5, p. 1287–1319, 2010.
UFV, C.; UFLA, F. Mapa de solos do Estado de Minas Gerais. **Universidade Federal de Viçosa**, p. 49, 2010.
VELDMAN, J. W. et al. Comment on "The global tree restoration potential". **Science**, v. 366, n. 6463, p. eaay7976, 2019.
VELOSO, G. A. et al. Modelling gross primary productivity in tropical savanna pasturelands for livestock intensification in Brazil. **Remote Sensing Applications: Society and Environment**, v. 17, p. 100288, 2020.
VELOSO, G. A.; FERREIRA, M. E.; DA SILVA, B. B. Determinação da evapotranspiração real diária em áreas irrigadas do projeto Jaíba (Minas Gerais, Brasil), mediante imagens Landsat 5-TM. **Cerrados**, v. 15, n. 1, p. 53–76, 2017.
VELOSO, G. A.; SILVA, L. A. P. DA; FERREIRA, M. E. Análise Do Balanço De Radiação E Energia Em Áreas De Veredas No Norte De Minas Gerais, Bioma Cerrado. **Revista Cerrados**, v. 18, p. 220–247, 2020a.
VELOSO, G. A.; SILVA, L. A. P. DA; FERREIRA, M. E. Análise do Balanço de Radiação e Energia em Áreas de Veredas no Norte de Minas Gerais, Bioma Cerrado. **Revista Cerrados**, v. 18, n. 1, p. 220–247, 2020b.
VENANCIO, L. P. et al. **Evapotranspiration mapping of commercial corn fields in Brazil using SAFER algorithmScientia Agricola**scielo, , 2020.
WANG, W. et al. Changes in reference evapotranspiration across the Tibetan Plateau: Observations and future projections based on statistical downscaling. **Journal of Geophysical Research: Atmospheres**, v. 118, n. 10, p. 4049–4068, 2013.
XIONG, Y. et al. The impacts of rapid urbanization on the thermal environment: A remote sensing study of Guangzhou, South China. **Remote sensing**, v. 4, n. 7, p. 2033–2056, 2012.
YU, H.; JIANG, S.; LAND, K. C. Multicollinearity in hierarchical linear models. **Social science research**, v. 53, p. 118–136, 2015.
ZEPPETELLO, L. V. et al. Large scale tropical deforestation drives extreme warming. **Environmental Research Letters**, 2020.

ZHANG, Y.; ODEH, I. O. A.; HAN, C. Bi-temporal characterization of land surface temperature in relation to impervious surface area, NDVI and NDBI, using a sub-pixel image analysis. **International Journal of Applied Earth Observation and Geoinformation**, v. 11, n. 4, p. 256–264, 2009.